A variable step size fuzzy MPPT controller improving energy conversion of variable speed DFIG wind turbine

A. Harrag [1,2*] and S. Messalti [3]

[1] Physics Department, Faculty of Sciences
Ferhat Abbas University Setif 1, El Bez, 19000 Setif, Algeria
[2] CCNS Laboratory, Electronics Department,
Faculty of Technology, Ferhat Abbas University, 19000 Setif, Algeria
[3] Electrical Engineering Department,
Faculty of Technology, Mohamed Boudiaf University, 28000 M 'Sila, Algeria

(reçu le 03 Avril 2017 - accepté le 30 Juin 2017)

Abstract - *With the world's fastest growing rate and the prominent part of installed renewable energy sources, it is clear that wind is now a mainstream source of energy supply that will play a leading role in the proclaimed fight against climate change. But becoming mainstream means also assuming new responsibilities, including ensuring the reliable and cost-effective functioning of the overall energy system. In this context, this paper deals with the problem of extracting the wind turbine maximum power, power that depends on the random nature of wind speed and the nonlinear characteristic P = f(w) making it more difficult to extract. For this task, we propose a variable step size fuzzy maximum power point tracking controller. The proposed controller is tested on wind turbine based on a doubly-fed induction generator controlled by a field-oriented control implemented using Matlab/Simulink environment. Simulation results are presented showing a net improvement using the proposed MPPT to converge toward the optimal point with good accuracy and low oscillations around the MPP point achieving better performances.*

Résumé - *Avec le taux de croissance le plus rapide au monde et la part dominante des sources d'énergie renouvelables installées, il est clair que le vent est maintenant une source d'approvisionnement en énergie qui jouera un rôle de premier plan dans la lutte proclamée contre le changement climatique. Mais le fait de devenir grand public implique également de nouvelles responsabilités, notamment en assurant le fonctionnement fiable et rentable du système énergétique global. Dans ce contexte, cet article traite le problème de l'extraction de la puissance maximale de l'éolienne, la puissance qui dépend de la nature aléatoire de la vitesse du vent et de la caractéristique non linéaire P = f(w), ce qui la rend plus difficile à extraire. Pour cela, nous proposons un contrôleur de suivi de point de puissance maximum flou à pas variable. Le contrôleur proposé est testé sur l'éolienne à base de DFIG contrôlé par flux orienté est implémenté sous l'environnement Matlab/Simulink. Les résultats de la simulation sont présentés montrant une amélioration nette en utilisant le MPPT proposé pour converger vers le point optimal avec une bonne précision et de faibles oscillations autour du point de MPP pour obtenir de meilleures performances.*

Key words: DFIG - Fuzzy logic - MPPT - Perturbe & Observe - Tip speed ratio - Wind turbine.

1. INTRODUCTION

The earth's fossil energy resources are limited. The global oil, gas and coal production will come beyond their peak in the next decades. At the same time there is strong political opposition against strengthening nuclear power in many parts of the world. In this scenario renewable energies will have to contribute more and more to the world's ever rising need of energy in the future. Renewable are climate-friendly forms of energy, due to the absence of emissions detrimental to the environment. The savings

*a.b.harrag@gmail.com

especially in carbon-dioxide and sulphur dioxide emissions are a significant advantage over fossil power. Hence a renewable energy will play a leading role in the proclaimed fight against climate change [1, 2].

Last year, a new record renewable power capacity of more than 140 GW was installed and more than 40 % of that capacity came from wind. That deployment was accompanied by record low prices for forthcoming renewable electricity, in some cases, wind onshore is already the cheapest electricity generation option and costs are continuing to decline. As consequence, wind energy is playing an increasingly important role in the supply of energy of most industrialized countries. Its share of the electrical generation is expected to continue to increase for many years to come.

In the past two decades, the global wind energy capacity has increased rapidly: breaking the 50 GW in 2014 and reached another record in 2015 with 63 GW as annual installations (22% increase), bringing to 433 GW of wind power spinning around the globe (17% increase) (figure 1). With these statistics, wind energy is now considered as the world's fastest growing energy source. In addition, the wind power supplied more new power generation than any other technology in 2015 [3].

Wind energy conversion system (WCES) comprise generally a wind turbine that converts the mechanical energy, issued from the wind conversion by the rotor blades, to electrical one through electrical generator, and power electronic converters that control the aero-generator. According to the rotor speeds, we use (or not) gearbox to increase speeds required by electrical generator. The turbine control includes two major parts: i) power control, in case of wind power less than rated, the blades are fixed to capture the maximum wind power and turbine speed will be controlled by adjusting electrical power; and ii) pitch control, in case of wind power above rated, the rotor speed will be controlled by the pitch for full power operation, with transient speed being allowed to rise above the reference [4].

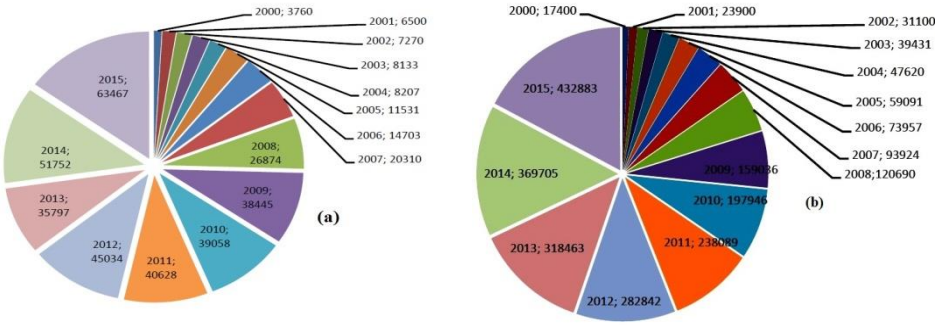

a) Global annual b) Global cumulative [5]

Fig. 1: Installed wind capacity 2000-2015

The output power of wind energy system varies depending on the random nature wind speed. In addition, due to the nonlinear characteristic of the wind turbine, it is difficult to maintain the maximum power output of the wind turbine for all wind speed conditions. Therefore, over the years, several maximum power point tracking (MPPT) algorithms have been developed to track the maximum power point of the wind turbine. Among them:

The perturbation and observation (P&O) [6, 7] as well as the hill climb searching (HCS) algorithm[8, 9], in which the control efforts to climb the $P_m = (V_m)$ curve in

the direction of increasing P_m, by varying the rotational speed periodically with a small incremental step in order to reduce the oscillation around the maximum power point (MPP). In these algorithms, there is a trade-off between the rate of response and the amount of oscillations under steady state conditions. To overcome this trade-off, the step size of varying amplitude can be applied [10, 11].

The tip speed ratio (TSR) control method regulates the tip speed ratio to maintain it to an optimal value, at which the rotational speed is optimum and the power extracted is maximum. This control requires the knowledge of wind speed, the turbine speed, and the reference optimal point of the TSR that drives the reference power [12].

Power signal feedback (PSF) strategy regulates the turbine power to maintain it to an optimal value, keeping the power coefficient Cp always at its maximum value corresponding to the optimum tip speed ratio. This method requires the knowledge of the wind turbine and maximum power curve [13]. In the same way, optimal torque control (OTC) is a slight variant of PSF algorithm. It adjusts the generator torque to its optimal at different wind speeds. The OTC method requires the knowledge of turbine characteristics ($C_{p\max}$ and k_{opt}) [14].

In this paper, a new variable step size fuzzy MPPT controllers has been proposed and investigated. The fuzzy MPPT requires as inputs for the fuzzy logic controller (FLC) the measurements of the power variation (dP) and speed variation (dw). The proposed fuzzy MPPT controller is tested on wind turbine based on a doubly-fed induction generator (DFIG) controlled by a field-oriented control strategy. Simulation results are presented showing a net improvement using the proposed MPPT to converge toward the optimal point.

The rest of this paper is organized as follows: Section 2 describes the DFIG wind turbine modeling including the wind turbine model, the DFIG model and the DFIG control strategy. The proposed variable step size fuzzy MPPT controller is detailed in Section 3. The simulation results and discussion are presented in Section 4. Finally, Section 5 concludes the paper giving some comments and future directions.

2. MODELLING OF DFIG WIND TURBINE

2.1 Wind turbine model

The principle of wind turbines in power generation is transformation of the air kinetic energy into rotating mechanical power of the turbine rotor blades. The basic formulation for the power in the wind in a location A, perpendicular to the wind blowing direction is given by the formula [15, 16]:

$$P = \frac{1}{2}.\rho.A.C_p.v^3 \tag{1}$$

where, P is the power; ρ is the air density; v is the wind speed; A is the turbine swept area; C_p is the power coefficient, which describes the fraction of the wind captured by a wind turbine.

According to Betz rules, the value of the power coefficient features a theoretic limit connected with 59.7 %.

C_p is often given as a function of the tip speed ratio λ defined by:

$$\lambda = \frac{R\,.\,\Omega_t}{v_{wind}} \tag{2}$$

The power coefficient C_p defined as a measurement of how the wind turbine converts the energy in the wind into electricity can be expressed power coefficient with different expressions [17, 18]. The power coefficient C_p in terms of TSR λ and pitch angle beta β for turbine 3 MW [19] is,

$$C_p(\lambda,\beta) = \left(0.35 - 0.0167(\beta - 2)\right)\sin\left(\frac{\pi(\lambda + 0.1)}{14.34 - 0.3(\beta - 2)}\right) - \ldots - \left(0.00184(\lambda - 3)(\beta - 2)\right) \quad (3)$$

Turbine torque is,

$$C_t = \frac{P_t}{\Omega_t} = \frac{1}{2\lambda} \times C_p(\lambda,\beta) \times \rho\pi R^3 v_{wind}^2 \quad (4)$$

Through the gearbox, the low-shaft speed Ω_t is increased by the gearbox ratio G to obtain the generator speed Ω_{mecg},

$$\Omega_{mecg} = G \times \Omega_t \quad (5)$$

The mechanical power converted by a wind turbine is dependent on the coefficient $C_p(\lambda,\beta)$ is given by,

$$P_{mg} = \frac{1}{2} \times C_p(\lambda,\beta) \times \rho\pi R^3 v_{wind}^2 \quad (6)$$

The characteristics of the typical captured output power for different pitch angles β (2, 4 to 14) are shown in figure 2.

From figure 2, we can see that captured wind turbine output power is dependent on pitch angle. The power coefficient-speed ratio ($C_p - \lambda$) characteristic presents a unique maximum point ($C_{p\max} - \lambda_{opt}$) for each pitch angle at which the turbine output power is maximum. As consequence, for each wind velocity exists only one turbine speed that provides a maximum output power as shown in figure 4.

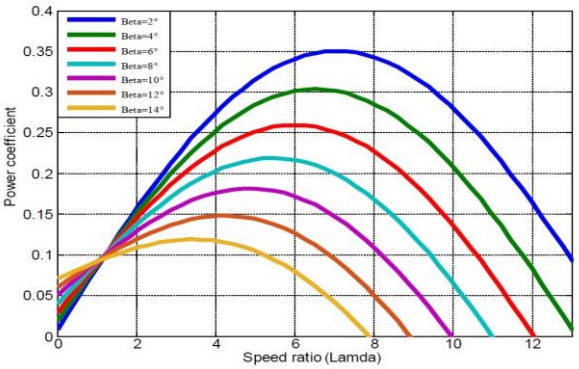

Fig. 2: Power coefficients versus speed ratio for turbine 3 MW [19]

2.2 DFIG model

The most common variable-speed wind turbines are the doubly fed induction generator, which offers high efficiency over a wide range of wind speeds as well as the

ability to supply power at a constant voltage and frequency while the rotor speed varies. This technology consists of a wound rotor induction generator and a back-to-back power converter placed into the rotor of the machine while the stator is directly connected to the grid.

The power converter allows for the machine to be controlled between sub-synchronous speed and super-synchronous speed, usually, a variation from -40% to +30% of synchronous speed is chosen. This converter capacity is designed to handle 20–30% of the machine rate, which is beneficial both economically and technically [20-22].

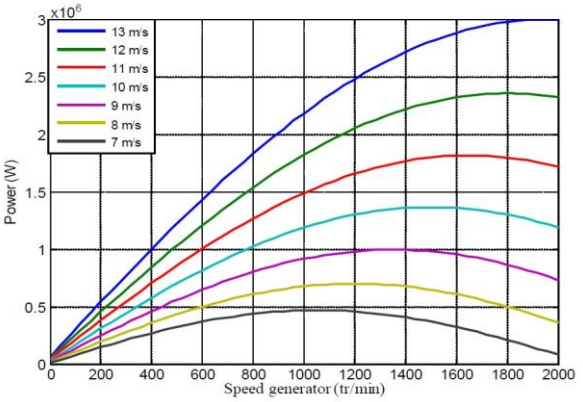

Fig. 3: Power versus rotational speed of generator for turbine 3 MW [19]

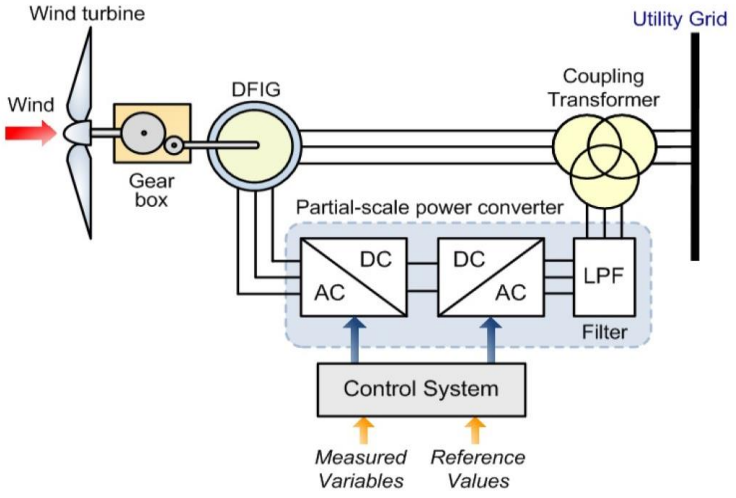

Fig. 4: The Wind turbine based on DFIG

The DFIG dynamic model in Park's reference is expressed as follows [23],

$$\begin{cases} V_{ds} = R_s.I_{ds} + \dfrac{d\phi_{ds}}{dt} - \omega_s.\phi_{qs} \\ V_{qs} = -R_s.I_{qs} + \dfrac{d\phi_{qs}}{dt} + \omega_s.\phi_{ds} \\ V_{dr} = R_r.I_{dr} + \dfrac{d\phi_{dr}}{dt} - \omega_r.\phi_{qr} \\ V_{qr} = R_r.I_{qr} + \dfrac{d\phi_{qr}}{dt} - \omega_r.\phi_{dr} \end{cases} \quad (7)$$

Flux linkage equations are obtained from,

$$\begin{cases} \phi_{ds} = -L_s.I_{ds} + M.I_{dr} \\ \phi_{qs} = -L_s.I_{qs} + M.I_{qr} \\ \phi_{ds} = -L_r.I_{dr} - M.I_{ds} \\ \phi_{ds} = -L_r.I_{qs} - M.I_{qr} \end{cases} \quad (8)$$

Electromagnetic torque equation is,

$$C_{em} = p\frac{M}{L_s}\left(\varphi_{qs}.i_{dr} - \varphi_{ds}.i_{qr}\right) \quad (9)$$

The associated motion equation is,

$$J\frac{d\Omega}{dt} = C_{em} - C_r - f\,\Omega \quad (10)$$

2.3 DFIG control

To guarantee an uncoupled control of the stator active and reactive power vector in the synchronous reference frame whose d axis is a ligne d with the stator flux vector, the DFIG model can be described by the following state equations [24, 25],

$$\phi_{ds} = \phi_s \quad \text{and} \quad \phi_{qs} = 0 \quad (11)$$

Replacing (11) in equations (8), (7) and (9), we obtain,

$$\begin{cases} \phi_s = -L_s.I_{ds} + M.I_{dr} \\ 0 = -L_s.I_{qs} + M.I_{qr} \end{cases} \quad (12)$$

$$\begin{cases} V_{ds} = R_s.I_{ds} + \dfrac{d\phi_s}{dt} \\ V_{qs} = R_s.I_{qs} + \omega_s.\phi_s \end{cases} \quad (13)$$

$$C_{em} = -p\frac{M}{L_s}\varphi_{ds}.i_{qr} \quad (14)$$

By neglecting the stator windings resistance, the stator voltage voltages equation (13) become,

$$\begin{cases} V_{ds} = 0 \\ V_{qs} = V_s = \omega_s.\phi_s \end{cases} \quad (15)$$

The relation between the stator and rotor currents is,

$$\begin{cases} I_{ds} = -\frac{M}{L_s}.I_{dr} - \frac{\phi_s}{t} \\ V_{qs} = \frac{M}{L_r}.I_{qr} \end{cases} \quad (16)$$

The stator active and reactive power are controlled by,

$$\begin{cases} P_s = V_s.I_{qs} = -\frac{\omega_s \cdot \phi_s}{L_r} I_{qr} \\ Q = V_s.I_{ds} = --\frac{\omega_s \cdot \phi_s.M}{L_s} I_{dr} + \frac{\omega_s.\phi_2^2}{L_s} \end{cases} \quad (17)$$

Substituting (16) in (7), we obtain,

$$\begin{cases} \phi_{dr} = \left(L_r - \frac{M^2}{L_s} \right) I_{dr} + \frac{V_s^2}{L_s \omega_s} \\ \phi_{qr} = \left(L_r - \frac{M^2}{L_s} \right) I_{qr} \end{cases} \quad (18)$$

Substituting (18) in (8), we obtain,

$$\begin{cases} V_{dr} = R_r I_{dr} + \left(L_r - \frac{M^2}{L_s} \right) \frac{d I_{dr}}{dt} - g\omega_s \left(L_r - \frac{M^2}{L_s} \right) I_{qr} \\ V_{qr} = R_r I_{qr} + \left(L_r - \frac{M^2}{L_s} \right) \frac{d I_{qr}}{dt} + g\omega_s \left(L_r - \frac{M^2}{L_s} \right) I_{dr} + g\omega_s \frac{M\phi_s}{L_s} \end{cases} \quad (19)$$

where g is the slip of the induction machine and $\omega_r = g\omega_s$.

In steady state operation the voltage expressions are,

$$\begin{cases} V_{dr} = R_r I_{dr} - g\omega_s \left(L_r - \frac{M^2}{L_s} \right) I_{qr} \\ V_{qr} = R_r I_{qr} + g\omega_s \left(L_r - \frac{M^2}{L_s} \right) I_{dr} + g\omega_s \frac{M\phi_s}{L_s} \end{cases} \quad (20)$$

3. PROPOSED VARIABLE STEP FUZZY MPPT

3.1 Fuzzy logic overview

The application of fuzzy logic has become more popular with the utilization of microcontrollers [26, 27**]**. Fuzzy logic controllers have the benefits of operating with general inputs, not needing associate correct mathematical model and handling nonlinearities mathematical logic management typically consists of three stages: fuzzification, rule base table operation, and defuzzification.

Throughout fuzzification, numerical input variables are regenerated into linguistic variables supported by a membership(figure 5). Fuzzy levels used are of the type: NB (Negative Big), NS (Negative Small), ZE (Zero), PS (Positive Small), and lead (Positive Big).

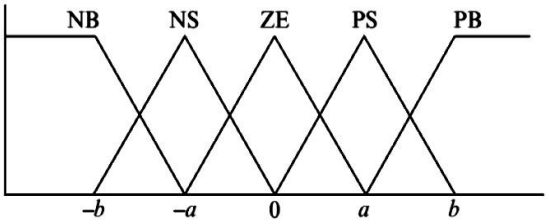

a , b are the membership values of the numerical variable

Fig. 5: Membership function for system variables

In the defuzzification stage, the fuzzy logic output is regenerated from a linguistic variable to a numerical variable still employing a membership operation as in figure 7 providing an analog output signal depending on the rule base table and inference method used.

3.2 MPPT controller

Despite the continuous development of new MPPT algorithms, the P&O algorithm remains by far the most used due to its simplicity and easy implementation. The principle can be described as follows: in the ascending phase of the $P_m(\omega_m)$ characteristics and considering a positive change of the rotational speed, the tracker generates a positive change ($d\omega_m > 0$), which results in an increase in the delivered mechanical power and change of the operating point X_i ($i = 1, 2, \ldots, n-1$).

In this case, the rotational speed and the P_m power increase up to a new point X_{i+1}. Similar steps with opposite direction can be done in the case of a decrease in the mechanical power, by setting $X = \omega_m$; the instantaneous rotational speed of the wind turbine follows the maximum power point according to a predetermined rotational speed and power values. Under these conditions, the tracker seeks the MPP permanently.

At specified wind speed, the desired mechanical power is the solution of the nonlinear equation given by ($dP_m / d\omega_m = 0$). However, the magnitude of the step size is the main factor determining the amplitude of oscillations that allows the convergence rate to the final response. Using a larger disturbance will lead to a higher value of oscillation amplitude around the peak point. Figure 6 show the principle of P&O algorithm.

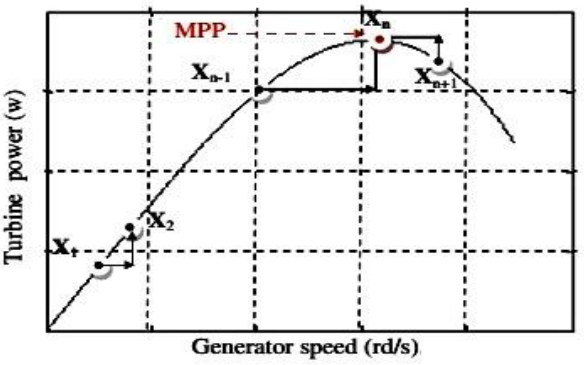

Fig. 6: P&O algorithm principle [4]

3.2.1 Variable step fuzzy MPPT implementation

In this study, a new variable step size fuzzy MPPT controllers has been proposed and investigated. The fuzzy MPPT requires as inputs for the fuzzy logic controller (FLC) the measurements of the power variation (dP_{wind}) and speed variation ($d\omega$). The fuzzy logic MPPT controller drives the speed as output as described in figure 7.

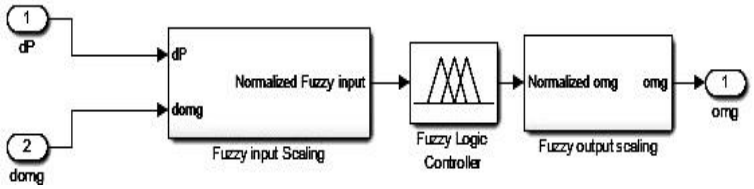

Fig. 7: Proposed fuzzy MPPT controller

The proposed fuzzy MPPT controller has been implemented under Matlab/Simulink environment (figure 8).

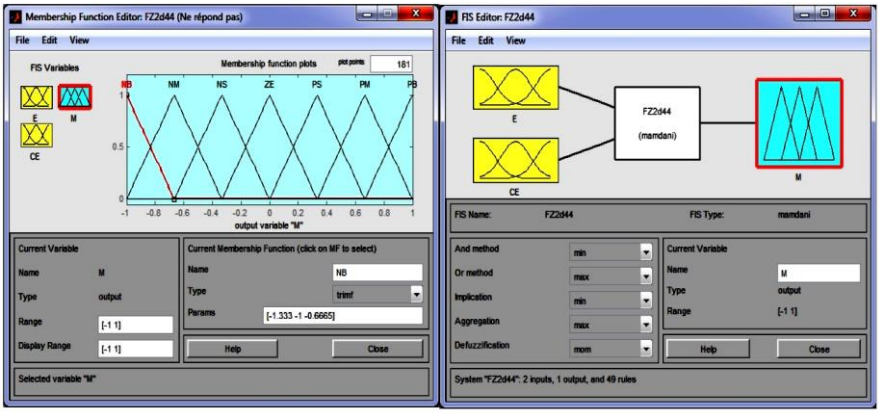

Fig. 8: Proposed fuzzy MPPT controller under Matlab/Simulink Environment

The output is computed using the rules base defined table in **Table 1**; while the figure 9 shows the fuzzy rules surface according to the defined rules base.

Table 1: Rules base

ce —e	NB	NM	NS	ZE	PS	PM	PB
NB	ZE	ZE	ZE	NB	NB	NB	NB
NM	ZE	ZE	ZE	NM	NM	NM	NM
NS	NS	ZE	ZE	NS	NS	NS	NS
ZE	NM	NS	ZE	ZE	ZE	PS	PM
PS	PM	PS	PS	PS	ZE	ZE	ZE
PM	PM	PM	PM	ZE	ZE	ZE	ZE
PB	PB	PB	PB	ZE	ZE	ZE	ZE

According to rules table, if the power (P_{wind}) increased, the operating point should be increased as well. However, if the power (P_{wind}) decreased, the speed should do the same.

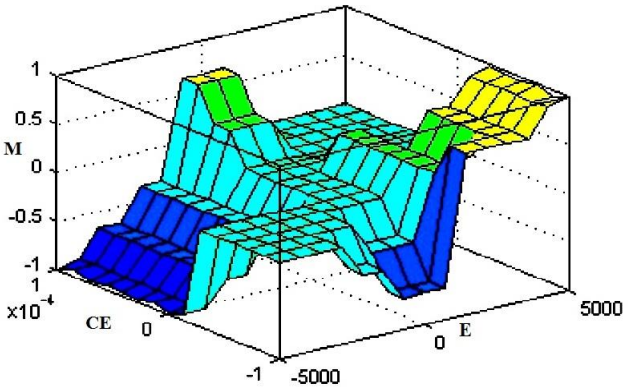

Fig. 9: Fuzzy rules surface

4. RESULTS AND DISCUSSIONS

The performance of the proposed variable step size fuzzy MPPT controller is presented. A wind energy conversion system based on 3 MW wind turbine connected to DFIG is employed. The rated system parameters are given in Appendix **A**. The simulation results have been carried out using Matlab/Simulink environment using the wind speed profile depicted in figure 10.

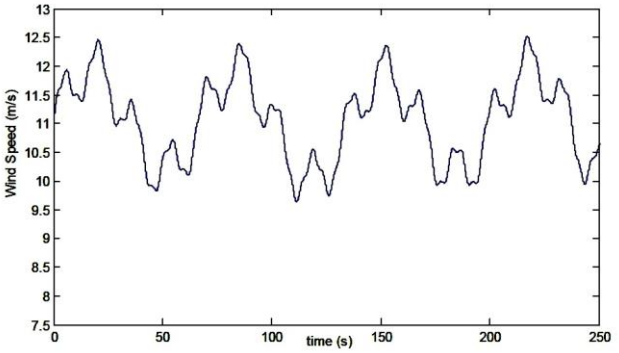

Fig. 10: Wind speed profile

The obtained results of the proposed variable step size fuzzy MPPT controller demonstrate a good performance to responds quickly to wind speed variations.

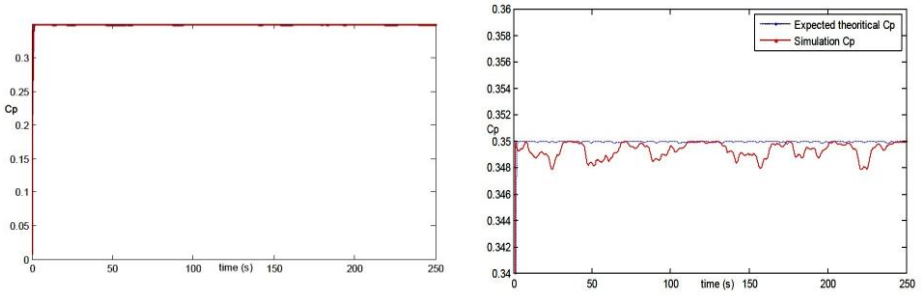

Fig. 11: Power coefficient C_p

Figures 11, 12 and 13 show the power coefficient, the output power and the optimal turbine rotational speeds, respectively.

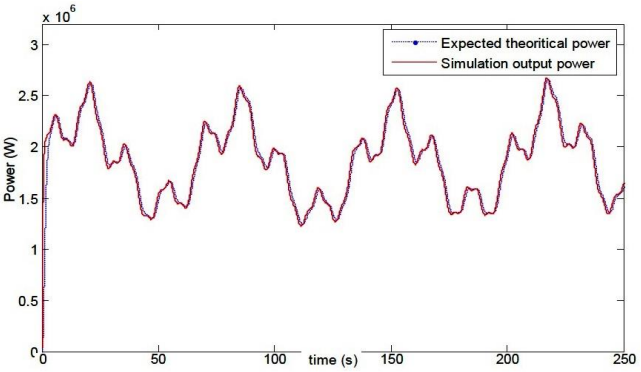

Fig. 12: Tracking MPPT power

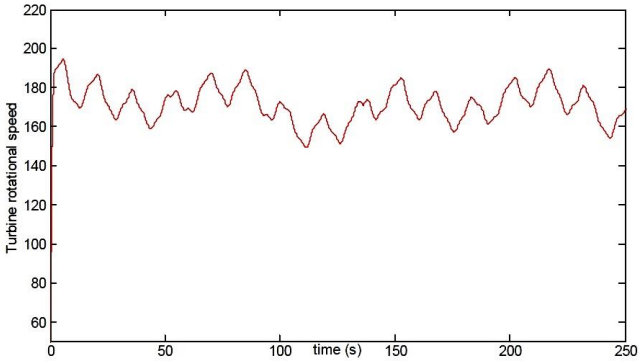

Fig. 13: Turbine rotational speed

We can see from figures 11 to 13 that the proposed variable step size fuzzy MPPT controls allows a good tracking accuracy and rapidity according to the wind profile. The computed output power is very close to the expected theoretical value. Figure 14 shows the normalized speed computed by the fuzzy MPPT controller.

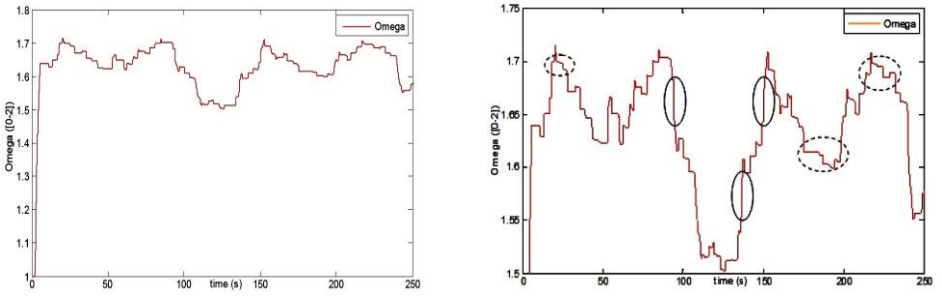

Fig. 14: Normalized speed

From figure 14, we can see clearly the variable step size with large step, if we are far from the MPP point (continuous line circles in figure 14**b**) and small step size if we are close to MPP point (dotted line circles in figure 14**b**).

From figures, it can be observed that the wind energy conversion system operates at its maximum power which it can be verified for nominal wind speed (13m/s). The power coefficient and output power correspond exactly at it nominal value 0.35 and 3MW, respectively. The results prove the effectiveness of the proposed variable step size fuzzy MPPT controller to track the maximum power delivered by the wind turbine according to the wind speed profile.

In addition, the proposed variable step size avoid the drawback of the fixed step size algorithms needing a trade off between the rate of response and the amount of oscillations under steady state conditions.

From the implementation consideration, the proposed fuzzy MPPT controller requires only the power and speed measurement with out the need of power coefficient information, the tip speed ratio or the characteristic curve of wind turbine.

5. CONCLUSION

In this paper, a new variable step size fuzzy MPPT controller based has been presented considering variable speed wind turbine driving doubly-fed induction generator.

Modelling and control strategies of the overall system have been developed and simulated using Matlab/Simulink environment under randomly and quickly varying wind speed. Simulation results confirm the high performance of proposed variable step size fuzzy MPPT controller showing a good concordance between simulation results and theoretically expected results.

The proposed MPPT controller requires only power and speed variation measurements to track effectively the maximum power without the need of power coefficient information, the tip speed ratio or the characteristic curve of wind turbine.

In addition, the variable step size allows the proposed fuzzy MPPT controller to track rapidly and with good accuracy and low oscillations around the MPP point achieving better performances.

APPENDIX A

Wind turbine parameters

$\rho = 1.225\ \mathrm{kg/m^3};\ R = 45;\ \beta = 2;\ G = 100;\ f_t = 0.0024;$

$\lambda_{max} = 7.07;\ t = \left(\frac{1.4\times10^{6}}{G^{2}} + J_g \right);\ C_{p\,max} = 0.35$

DFIG parameters

3 MW; 690V/15kV; 50 Hz; $N_m = 1440;\ m = 1;\ L_{fs} = 121\times10^{-6};$

$p = 2;\ L_{fr} = 57.3\times10^{-6};\ L_m = 12.12\times10^{-3};\ L_s = L_{fs} + L_m;$

$L_r = L_{fr} + m^2 \times L_m;$

$M = m\times L_m;\ R_s = 0.00297;\ R_r = 0.00382;\ J_g = 114;\ f_g = 0.0071.$

REFERENCES

[1] S.R. Bull, '*Renewable Energy Today and Tomorrow*', Proceedings IEEE, Vol. 89, 2001, N°8, pp. 1216 -1226, 2015.

[2] M. Stiebler, '*Wind Energy Systems for Electric Power Generation*', Green Energy and Technology, Springer-Verlag Berlin Heidelberg, 2008.

[3] International Energy Agency IEA Wind 2015 – Annual Report URL: http://www.ieawind.org

[4] D. Rekioua, '*Wind Power Electric Systems*', Green Energy and Technology, Springer-Verlag London 2014.

[5] GWEC – Global Wind 2015 *Report Global Status of Wind Power in 2015*. URL: http:// www.gwec.net.

[6] N. Femia, D. Granozio, G. Petrone, G. Spagnuolo and M. Vitelli, '*Predictive & Adaptive MPPT Perturb and Observe Method*', IEEE Transactions on Aerospace and Electronic Systems, Vol. 43, N°3, pp. 934 – 950, 2007.

[7] B. Masood, M.S. Siddique, R.M. Asif and M. Zia-ul-Haq, '*Maximum Power Point Tracking using Hybrid Perturb & Observe and Incremental Conductance Techniques*', 4th International Conference Engineering Technopreneush, pp. 354 - 359, 2014.

[8] S. Lalouni, D. Rekioua, K. Idjdarene and A. Tounzi, '*Maximum Power Point Tracking Based Hybrid Hill-climb Search Method Applied to Wind Energy Conversion System*', Renewable Energy Devices and System, Research, N°8-10, pp. 1028 - 1038, 2015.

[9] I. Houssamo, F. Locment and M. Sechilariu, '*Experimental Analysis of Impact of MPPT Methods on Energy Efficiency For Photovoltaic Power Systems*', International Journal of Electric Power Energy System, Vol. 46, pp. 98 - 107, 2013.

[10] C.A. Ramos-Paja, A.J. Saavedra-Montes and E. Arango, '*Maximum Power Point Tracking in Wind Farms by Means of a Multi Variable Algorithm*', Workshop on Engineering Applications, pp. 1 - 6, 2012.

[11] A. Harrag and S. Messalti, '*Variable Step Size Modified P&O MPPT Algorithm using GA-Based Hybrid Offline/Online PID Controller*', Renewable Sustainable Energy Review, Vol. 49, pp 1247 -1260, 2015.

[12] M. Nasiri, J. Milimonfared and S.H. Fathi, '*Modeling, Analysis and Comparison of TSR and OTC Methods for MPPT and Power Smoothing in Permanent Magnet Synchronous Generator-Based Wind Turbines*', Energy Conversion and Management, Vol. 86, pp. 892 - 900, 2014.

[13] G. Hua and Y. Geng, '*A Novel Control Strategy of MPPT Taking Dynamics of Wind Turbine into Account*', 37th IEEE Power Electronics Specialist Conference, pp. 1- 6, 2006.

[14] Y. Zhao, C. Wei, Z. Zhang and W. Qiao, '*A Review on Position / Speed Sensorless Control for Permanent-Magnet Synchronous Machine-Based Wind Energy Conversion Systems*', IEEE Journal of Emerging and Selected Topics in Power Electronics, Vol. 1, N°4, pp. 203 - 216, 2013.

[15] J.G. Njiri and D. Söffker, '*State-of-the-Art in Wind Turbine Control: Trends and Challenges*', Renewable and Sustainable Energy Reviews, Vol. 60, pp. 377 - 393, 2016.

[16] M. Lydia, S.S. Kumar, A.I. Selvakumar and G.E.P. Kumar, '*A comprehensive review on wind turbine power curve modeling techniques*', Renewable Sustainable Energy Review, Vol. 30, pp. 452 - 460, 2014.

[17] O. Anaya-Lara, N. Jenkins, J. Ekanayake, P. Cartwright and M. Hughes, '*Wind Energy Generation: Modelling and Control*', West Sussex, UK: Wiley, 2009.

[18] J.F. Manwell, J.G. McGowan and A.L. Rogers, '*Wind Energy Explained: Theory, Design and Application*', Wiley, London, 2010.

[19] A. Gaillard, '*Système Eolien Basé sur une MADA Contribution à l'Etude de la Qualité de l'Energie Electrique et de la Continuité de Service*', Ph.D. Dissertation, Henri Poincaré University, Nancy-I, 2010.

[20] E.E. Ozsoy, E. Golubovic, A. Sabanovic, M. Gokasan and S. Bogosyan, '*A Novel Current Controller Scheme for Doubly Fed Induction Generators*', Automatika, Vol. 56, N°2, pp. 186 - 195, 2015.

[21] S. Abdeddaim and A. Betka, '*Optimal Tracking and Robust Power Control of the DFIG Wind Turbine*', Electrical Power and Energy Systems, Vol. 49, pp. 234 - 242, 2013.

[22] S.Y. Yang, Y.K. Wu, H.J. Lin, and W.J. Lee, '*Integrated Mechanical and* Industry Applications, Vol. 50, N°3, pp. 2090 - 2102, 2014.

[23] P.K. Gayen, D. Chatterjee and S.K. Goswami, '*Stator Side Active and Reactive Power Control with Improved Rotor Position and Speed Estimator of a Grid Connected DFIG (doubly-fed induction generator)*', Energy, Vol. 89, N°C, pp. 461 - 472, 2015.

[24] S. Abdeddaim, A. Betka, S. Drid and M. Becherif, '*Implementation of MRAC Controller of a DFIG Based Variable Speed Grid Connected Wind Turbine*', Energy Conversion and Management, Vol. 79, pp. 281 - 288, 2014.

[25] W. Pedrycz, '*Fuzzy Control and Fuzzy Systems*', (2 Ed.). Research Studies Press Ltd, 1993.

[26] A.G. Aissaoui, A. Tahour, N. Essounbouli, F. Nollet, M. Abid and M.I. Chergui, '*A Fuzzy-PI Control to Extract an Optimal Power from Wind Turbine*', Energy Conversion and Management, Vol. 65, pp. 688 - 696, 2013.